The Egyptian Journal of Hospital Medicine (January 2023) Vol. 90, Page 668-678

Histological and Ultrastructural Changes of Cefepime on the Kidney in The Adult Albino Rats

Mohammed Hegazy Hassan Ali [1,*]; Mohamed Al-Hady Zahran [2]; Gamal M. Aboul-Hassan[1]
[1] Departments of Anatomy, Faculty of Medicine, Al-Azhar University, Assuit, Egypt
[2] Departments of Anatomy, Faculty of Medicine, Al-Azhar University, Cairo, Egypt
***Corresponding Author:** Mohammed H. H. Ali, **Mobile:** +201550624531, **E-mail:** drhegazy2008@gmail.com

ABSTRACT
Background: The cephalosporins are β-lactam antibiotics that, in terms of both structure and function, are very similar to penicillin. Cefepime is one of the most widely used parenteral fourth generation cephalosporins with broad-spectrum action. The administration of a high dose of cefepime can exert a direct cytotoxic effect which accumulated in the tubular epithelial cells.
Objective: The present work aimed to reveal the histological and ultrastructural alterations in the kidney of the adult albino rats in relation to the dose of cefepime given. That's may give a new insight into the prophylaxis of cefepime nephrotoxicity.
Material and methods: 25 adult albino rats were divided into five equal groups. In group I (control group) each rat was injected intramuscularly with 1 ml isotonic saline solution /day for one week. Each rat of group II, III, IV and V was injected by cefepime intramuscularly in doses 50, 75, 100 and 125 mg/kg/day respectively for one week. After 2 months kidneys of rats were excised for routine histological and electron microscopic studies. **Results:** Intramuscular injection of cefepime led to histological and ultrastructural alterations of the cortex and medulla which were marked with increasing its concentration. Cytotoxic damage to the renal tubules, glomeruli and interstitium was obtained. The histological and ultrastructural changes in the kidney caused by cefepime were marked in group III, IV and V.
Conclusion: Cefepime nephrotoxicity were marked with increasing its concentration which proves that, cefepime nephrotoxicity in rats were dose related.
Keywords: Cefepime; cephalosporins; nephrotoxicity; kidneys.

INTRODUCTION

Various drugs or their metabolites are excreted by the kidney. Modifications in glomerular nephropathy, tubular damage or obstruction, kidney hemodynamics, and interstitial nephritis are the manifestations of nephrotoxicity [(1)].

The onset of many acute and chronic renal disorders is usually correlated with drug use. The two most common forms of tubulointerstitial compartment injury either acute tubular necrosis (ATN) or acute interstitial nephritis (AIN) are linked to nephrotoxicity. Additionally, the possibility of drug-induced glomerular diseases has been brought up in an increasing number of publications, including immune-mediated injury or even direct cellular injury. It is believed that an immune response is a part of the pathogenesis of AIN. Frequently, the development of that hypersensitive reaction involves cephalosporins, especially cefepime [(2)].

The development of cefepime was in 1990. Its antibacterial activity is close to that of third generation cephalosporins, however it has a significant level of beta-lactamase resistance. Furthermore, due to its high potency and broad spectrum, it is useful in treating a variety of serious illnesses, including septicemia, bacteremia, febrile neutropenia, and hospital-acquired pneumonia [(3)].

For an average adult with normal renal function, the recommended therapeutic dose of cefepime is 1-2 g/day intravenously. In child with febrile neutropenia, the dose is 50 mg/kg/day intravenously [(3)].

A rat model has been used to describe the dose-dependent feature of cefepime nephrotoxicity. As this antibiotic's concentration rises, it directly causes injury of the renal tubules, resulting in manifestations as proteinuria, glycosuria, and an increase in the urine salt excretion [(4)]. There have been reports of interstitial nephritis in association with cefepime [(5)].

This work aimed to investigate the histological and ultrastructural alterations in the kidney of the adult albino rats in rel/ation to the dose of cefepime administration.

MATERIAL AND METHODS

Experimental animals:

Twenty-five adult albino rats with average body weight 150 ± 40 g were purchased from the breeding unit of "Helwan Farm of experimental animals - VACSERA, Egypt". The study was done at faculty of medicine, Al-Azh ar University. The rats were kept for one week in standard cages with clear sides, controlled temperature (23± 3°C), humidity (approximately 60%), 12 hours of light and 12 hours of darkness, and access to food and water. Strict cleaning and care procedures were crucial for maintaining animals in good health.

Chemical material:

Cefepime 500 mg vial was obtained from "Pharco B International, Egypt". Its commercial name is "Cefepime". Each 1 ml contains 100 mg of cefepime. The

Received: 6/7/2022
Accepted: 11/9/2022

dose was calculated according to the average body weight rats and specified dose for each group.

Experimental design:

Rats were randomly divided into five groups (5 rats in each group). Each group was put in a separate cage and rats were injected as follows:

In group I (control): each rat was injected intramuscularly by 1 ml isotonic saline solution/day for one week.

In group II: each rat was injected by cefepime (50 mg/kg/day) [(3)] intramuscularly for one week.

In group III: rats were injected by cefepime intramuscularly (75 mg/kg/day) for one week.

In group IV: each rat was injected by cefepime intramuscularly (100 mg/kg/day) for one week.

In group V: each rat was injected by cefepime intramuscularly (125 mg/kg/day) for one week.

At the end of specified duration for injection, rats were sacrificed 24 hours after the last dose. On that day, the rats were anaesthetized with light ether inhalation then sacrificed using lethal dose of ether.

Kidney specimen's collection and light microscopic processing:

The abdomens of the deceased rats were cut midline, the viscera were pulled to one side to reveal the posterior abdominal wall, and fine dissection was performed around the abdominal aorta to adequately expose it and an excised kidney was fixed in 10% neutral buffered formalin then embedded in paraffin and lastly, sectioned at five microns, and stained with hematoxylin and eosin after being rinsed with saline [(6)].

Electron microscopic processing:

A kidney specimen (1 mm3 thickness) was fixed for 24 hours in 2.5% glutaraldehyde in phosphate buffer, washed with phosphate buffer for 20 minutes, and then post-fixed for 24 hours at 4 C° in a fume cupboard with osmium tetraoxide. The specimens were prepared for dehydration, infiltration and ultramicrotomy. Following that, the tissues were dyed with uranyl acetate and lead citrate for transmission electron microscope (TEM) processing [(7)].

Light microscopy was performed to evaluate the histological changes. Other ultrathin sections were studied by Zeiss EM 100 S transmission electron microscope at 60 KV at the "Regional Center for Fungi" at Al-Azhar University.

Ethical Approval

Ethical approval was taken from ethical committee of Faculty of Medicine, Al-Azhar University.

RESULTS

1. Light Microscopic Results:

Group I (control group):

Light microscopic sections the renal cortex of group I showed normal histological architecture of the cortex. Each glomerulus formed of a tuft of capillaries that surrounded by parietal layer (simple squamous epithelium) and visceral layer (podocytes) of Bowman's capsule. The space between the two layers of Bowman's capsule was called Bowman's space. The proximal convoluted tubules were normal and lined by simple cuboidal epithelium. The tubular lumina appeared narrow or filled because of the long microvilli of the free brush border. The distal tubules were normal and were lined by cuboidal epithelium (Fig. 1). The loops of Henle were normal and were lined by simple squamous epithelial cells (Fig. 1).

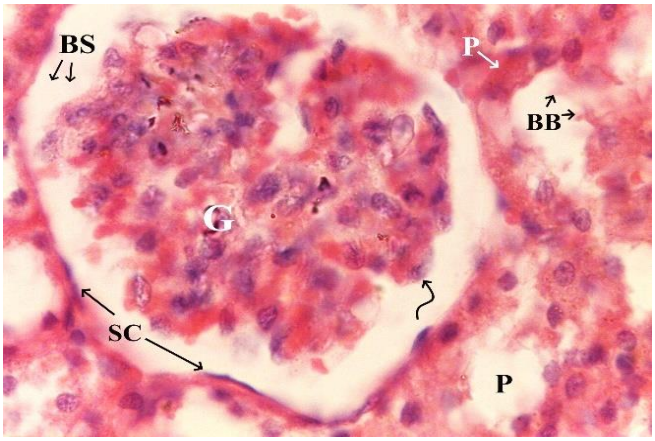

Fig. (1): Photomicrograph of a section in the cortical part of kidney of rat from control group reveals normal glomerulus (G) and normal Bowman's space (BS). Simple squamous cells (SC) form parietal layer of Bowman's capsule. Nuclei and cell bodies of the podocytes (curved arrow) bulge into the Bowman's space to form the visceral layer of Bowman's capsule. The lumen of proximal (P) convoluted tubule appear narrow, because of the long microvilli of the brush border (BB) (H. & E. x 1000).

Group II:

Minimal glomerular, tubular and interstitial alterations as follows:

The majority of glomeruli were normal. They were surrounded by normal Bowman's spaces; the remaining glomeruli were hypercellular and some had narrow Bowman's spaces while few were atrophied (Fig. 2).

The proximal tubules had dilated lumina, some had edematous epithelial lining, interrupted basement membrane and the cytoplasm of some tubules revealed large vacuoles. The tubular lumina contained cellular debris. Some of distal tubules have dilated lumina (Fig. 3).

The interstitium revealed patchy areas of inflammatory cellular infiltration and multiple areas of interstitial hemorrhage (Fig. 2).

The proximal and distal straight tubules in the outer medulla have edematous epithelial lining with detached epithelium at some areas and dropped out nuclei in their lumina. The inter-tubular blood capillaries of vasa recta were congested and filled with RBCs.

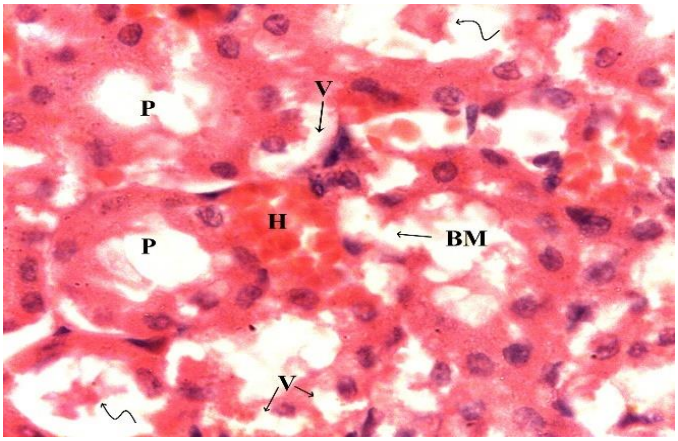

Fig. (2): Photomicrograph of a section in the cortical part of kidney of rat from group II reveals multiple proximal (P) tubules. The proximal tubules have edematous epithelial lining with large cytoplasmic vacuoles (V). Their tubular lumina are dilated and contain intra-luminal cellular debris (curved arrows). The tubular basement membrane (BM) is interrupted. The interstitium showing multiple areas of interstitial hemorrhage (H) (H. & E. x 1000).

Group III:

Glomerular, tubular, and interstitial alterations were increased as follows:

The majority were hypercellular and the remaining were atrophied and have dilated Bowman's spaces (Fig. 3).

The proximal tubules had dilated lumina, edematous epithelial lining and multiple cytoplasmic vacuoles in some tubules. Some of distal tubules have dilated lumina, edematous epithelial lining and dropped out cells in some tubules as a result of desquamation of epithelium Figs. 3 and 4).

The interstitium demonstrated multiple focal areas of interstitial hemorrhage, inflammatory cellular infiltration around the tubules (Figs. 3).

The inter-tubular blood capillaries of vasa recta in outer and inner medulla were congested and the outer portion of the renal medulla revealed tubules that had edematous epithelial lining with detached epithelium. The tubular basement membrane was interrupted and the type of tubules cannot be differentiated (Fig. 5).

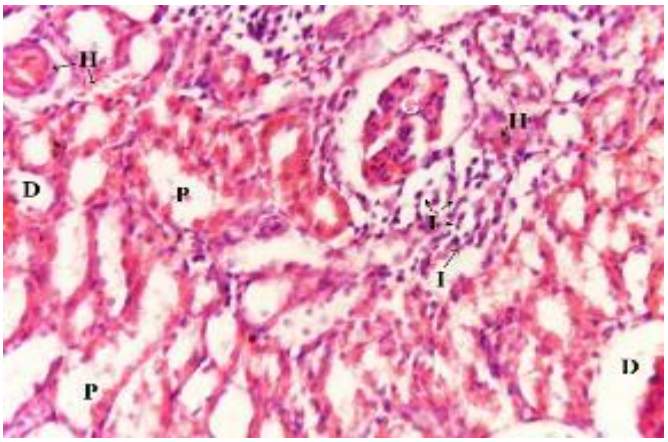

Fig. (3): Photomicrograph of a section in the cortical part of kidney of rat from group III showing hypercellular glomerulus (G) surrounded by large areas of marked interstitial inflammatory cellular infiltration (I). The interstitium showing focal areas of interstitial hemorrhage (H). Proximal (P) and distal tubules (D) have dilated lumina and edematous epithelial lining (H. & E. x 400).

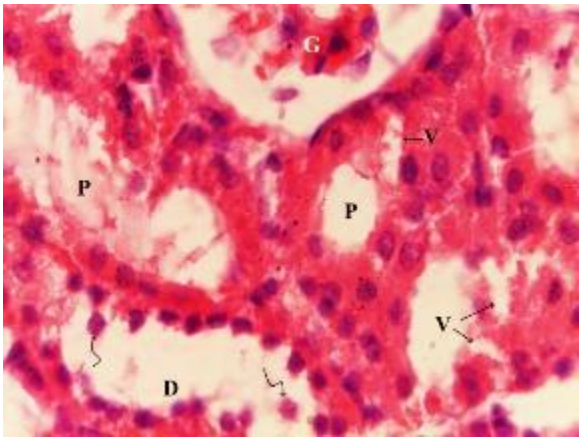

Fig. (4): Photomicrograph of a section in the cortical part of the kidney of rat from group III showing part of glomerulus (G). The proximal tubules (P) have edematous epithelial lining, cytoplasmic vacuoles (V) and dilated lumina. The distal tubules (D) have dilated lumina with dropped out cells (curved arrows) (H. & E. x 1000).

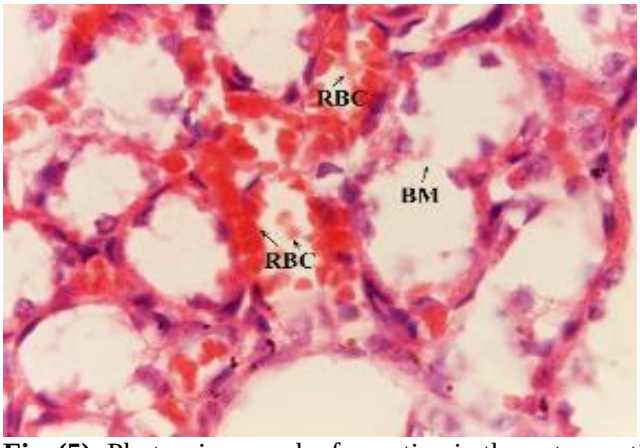

Fig. (5): Photomicrograph of a section in the outer portion of the renal medulla of rat from group III showing

transversely sectioned tubules. They have edematous epithelial lining with detached epithelium and the tubular basement membrane (BM) is interrupted and the type of tubules cannot be differentiated. The inter-tubular capillaries are congested and filled with RBCs (RBC) (H. & E. x 1000).

Group IV:

Glomerular, tubular and interstitial alterations were increased as follows:

All glomeruli were hypercellular and two types of glomeruli were noticed; the majority were surrounded by narrow Bowman's spaces. The remaining were atrophied and have dilated Bowman's spaces (Figs. 6 &7).

The proximal tubules had edematous epithelial lining and dilated lumina. Some tubules had desquamation of epithelium and multiple cytoplasmic vacuoles were noticed (Fig. 7). Some of distal tubules have dilated lumina with dropped out cells (Fig. 6).

Multiple areas of inflammatory cellular infiltration around the tubules were shown. The interstitium showed multiple areas of interstitial hemorrhage (Fig. 6).

The tubules in the outer medulla had edematous epithelial lining with detached epithelium and dropped out nuclei in the tubular lumina which cause the type of tubules cannot be differentiated. The inter-tubular blood capillaries are congested and filled with RBCs (Fig. 8).

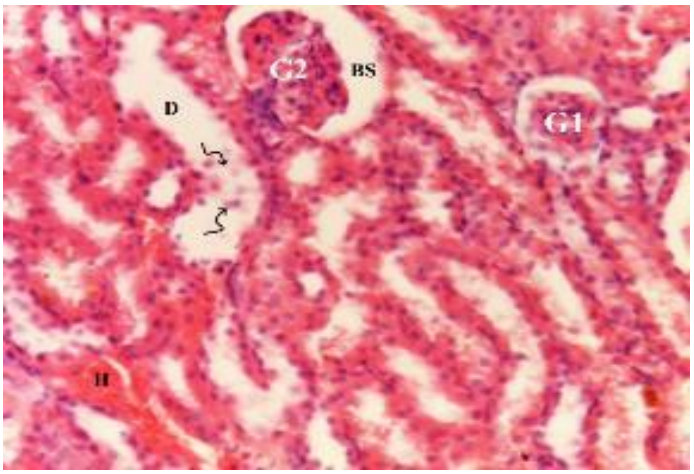

Fig. (6): Photomicrograph of a section in the cortical part of the kidney of rat from group IV showing hypercellular glomerulus (G1). Another glomerulus (G2) is atrophied and has dilated Bowman's space (BS). Some distal tubules (D) have dilated lumina and dropped out cells (curved arrows). The interstitium showing area of interstitial hemorrhage (H) (H. & E. x 400).

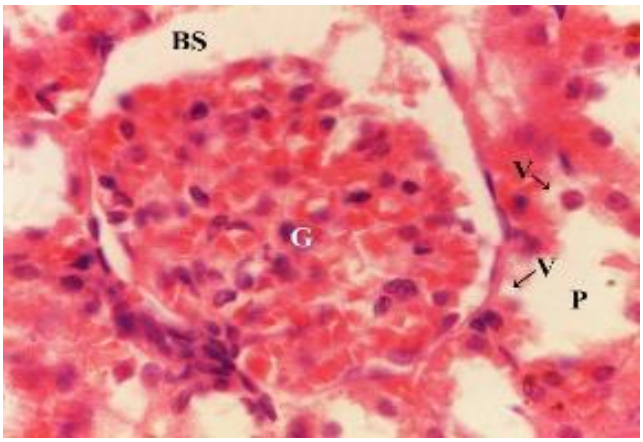

Fig. (7): Photomicrograph of a section in the cortical part of the kidney of rat from group IV showing renal glomerulus (G) has narrow Bowman's space (BS) in its lower half. The proximal tubules (P) have dilated lumina and edematous epithelial lining and cytoplasmic vacuoles (V) (H. & E. x 1000).

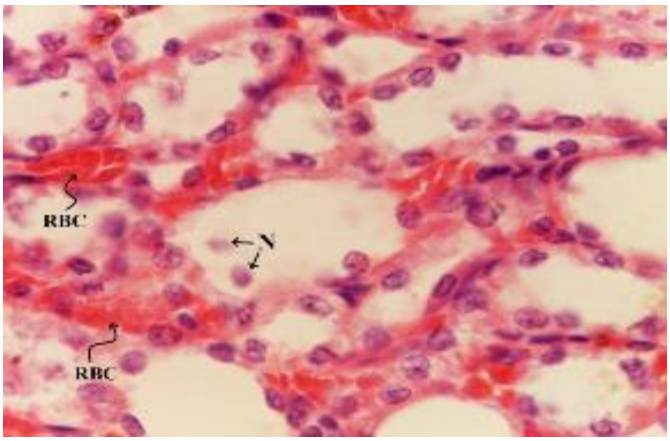

Fig. (8): Photomicrograph of a section in the outer portion of the renal medulla belonging to rat from group IV showing transversely sectioned tubules. They have edematous epithelial lining with detached epithelium which cause the type of tubules cannot be differentiated. Some nuclei (N) are dropped out in the tubular lumina. The blood capillaries are markedly congested and filled with RBCs (RBC) (H. & E. x 1000).

Group V:

Glomerular, tubular, and interstitial alterations were markedly increased as follows:

All glomeruli were hypercellular and some glomeruli were surrounded by narrow Bowman's spaces, but remaining glomeruli were atrophied and had dilated Bowman's spaces. Additionally, the parietal layers of Bowman's capsule of some glomeruli were interrupted and irregular (Fig. 9).

The proximal tubules had dilated lumina, edematous epithelial lining with marked desquamation of epithelium in some areas and multiple cytoplasmic vacuoles. Due to the desquamation and necrosis of the epithelium, certain

tubular lumina contained intra-luminal cellular debris. All distal tubules have dilated lumina (Figs. 9 and 10).
There were numerous regions of significant interstitial hemorrhage and inflammatory cellular infiltration in the interstitium. (Fig. 10). The tubules in the outer medullary region had edematous epithelial lining with detached epithelium and dropped out nuclei in the tubular lumina which cause the type of tubules cannot be differentiated.

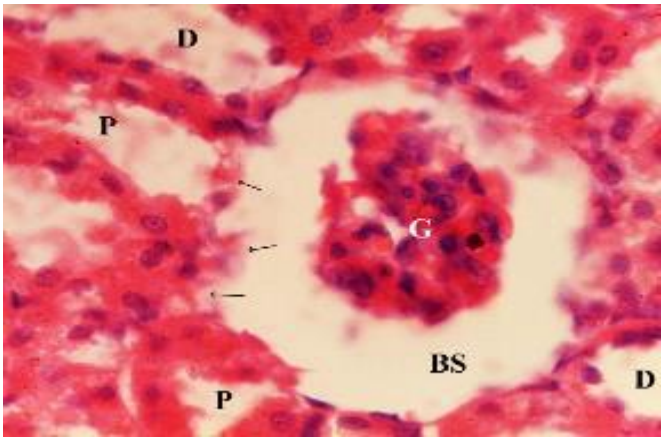

Fig. (9): Photomicrograph of a section in the cortical part of kidney of rat from group V showing atrophied glomerulus (G) has dilated Bowman's space (BS). The parietal layer of Bowman's capsule is interrupted and irregular (arrows). Proximal (P) and distal (D) convoluted tubules have dilated lumina (H. & E. x 1000).

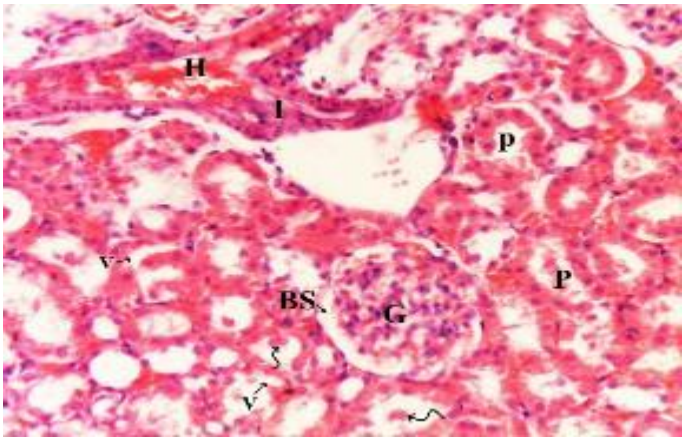

Fig. (10): Photomicrograph of a section in the cortical part of the kidney of rat from group V showing hypercellular glomerulus (G) has narrow Bowman's space (BS). Proximal tubules (P) have edematous epithelial lining with marked desquamation of epithelium and cytoplasmic vacuoles (V) at some areas. Their tubular lumina are dilated and contain intra-luminal cellular debris (curved arrows). The interstitium showing extensive interstitial hemorrhage (H) surrounded by inflammatory cellular infiltration (I) (H. & E. x 400).

2. Electron microscopic results:

Group I (control group):

Normal ultrastructural features of the glomerular capillary loops, lumen, endothelial inner layer, glomerular basement membrane, podocytes cell body and podocyte primary and secondary processes or pedicels. The extraglomerular mesangial cells were normal (Fig. 11). Normal proximal and distal tubular cells had normal euchromatic nuclei, intact cytoplasm containing many mitochondria and some lysosomes (Fig. 12)

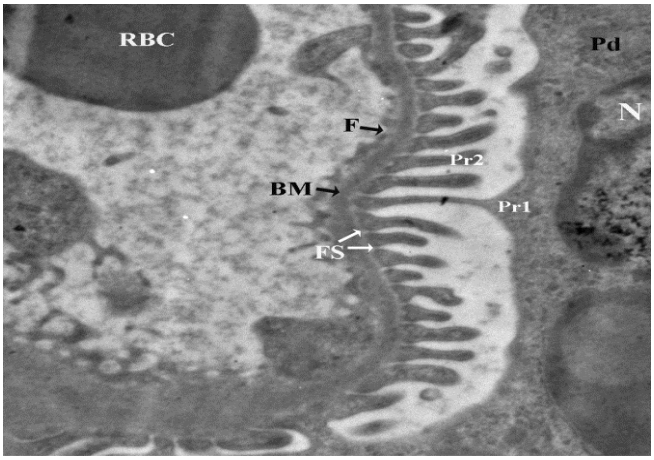

Fig. (11): Electron photomicrograph of a section in cortical part of kidney of rat from control group show glomerular capillary with overlying part of cell body of the podocyte (Pd) with its nucleus (N) and several primary processes (Pr1). Series of pedicels or secondary processes (Pr2) reach the capillary basement membrane (BM) and separated by the filtration slits (FS). At the inner side of the capillary basement membrane, the endothelium has pores so called fenestrated endothelium (F) of glomerular capillary. The capillary lumen contains RBC (RBC) (TEM. x 25000).

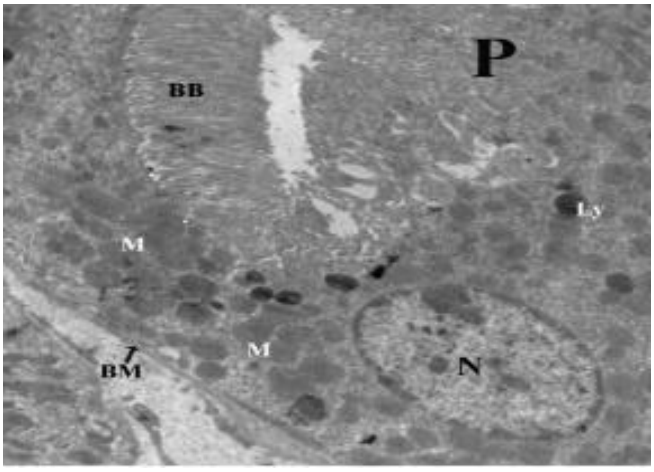

Fig. (12): Electron photomicrograph micrograph of a section in cortical part of the kidney of rat from control group showing a part of proximal convoluted tubule (P). The tubular cell has large round euchromatic nucleus (N)

and rest on normal thin intact basement membrane (BM). The cytoplasm containing many mitochondria (M) and some lysosomes (Ly). A brush border (BB) is clearly formed by the many microvilli at the luminal side (TEM. x 8000).

Group II:

Glomerular, tubular, and interstitial alterations were increased as follows:

The electron microscopic findings revealed occasional podocytes foot processes effacement and destructions, occluded filtration slits, thickened glomerular basement membrane and capillary endothelial degeneration with widening of their fenestrations (Fig. 13). The proximal tubular epithelial cells showed focal cytoplasmic vacuoles. Some nuclei were irregular and shrunken with loss of their peripheral chromatin. The apical brush border microvilli were varied from lost in some areas to mostly lost. The lumen of some tubules showed slugged materials (intra-luminal cellular debris) caused by desquamation and necrosis of epithelial lining (Fig. 14).

Most of distal tubular cells have normal euchromatic nuclei but other nuclei were shrunken, and the tubular lumen is occluded. (Fig. 15). The peritubular blood vessels were congested and the peritubular space revealed inflammatory cellular infiltration (Figs. 14).

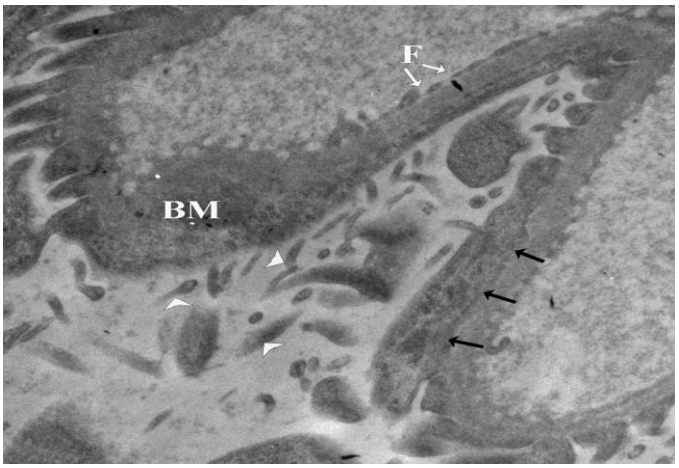

Fig. (13): Electron photomicrograph of glomerular capillary of cortical part of kidney of rat from group II showing foot processes effacement (black arrows) which occlude the filtration slits. Arrowheads point to microvillus transformation of destructed the pedicles of podocytes. The basement membrane (BM) is thickened with electron dense. There are widening of the fenestrations (F) of glomerular capillary endothelium (TEM. x 25000).

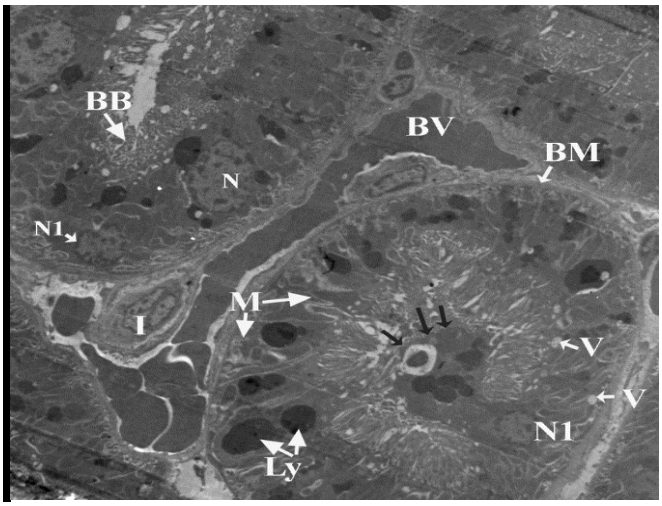

Fig. (14): Electron photomicrograph of a section in cortical part of kidney of rat from group II showing parts of proximal tubules (P). some tubular cells have normal round euchromatic nuclei (N), and the others are shrunken and irregular (N1). The cells rest on a thin intact basement membrane (BM). The cytoplasm containing many mitochondria (M), many lysosomes (Ly) and small vacuoles (V). The microvilli are intact and forming clearly obvious brush border (BB) except in some areas at which it completely disappeared (arrowheads). The lumen of one tubule shows intra-luminal cellular debris (arrows). The peritubular space show inflammatory cellular infiltration (I) and the peritubular blood vessel (BV) is congested and filled with RBCs (RBC) (TEM. x 3000).

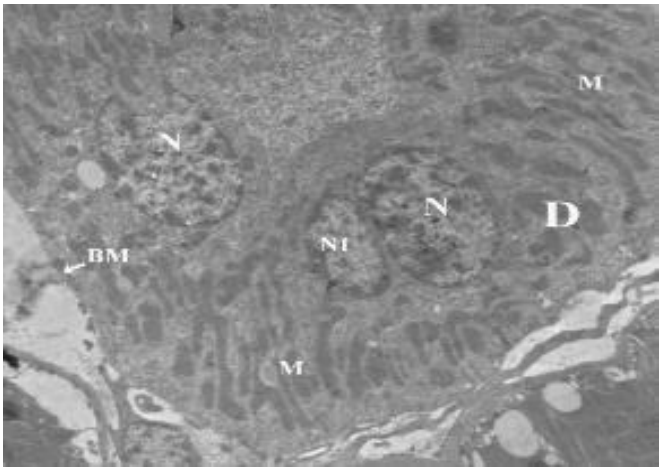

Fig. (15): Electron photomicrograph of a section in cortical part of kidney of rat from group II showing a part of distal tubule (D). Most of nuclei (N) are normal euchromatic, but one appears shrunken (N1). The basement membrane (BM) is intact. The cytoplasm containing many mitochondria (M) (TEM. x 6000).

Group III:
Glomerular, tubular and interstitial alterations were increased as follows:
Effacement of the podocyte foot processes around the glomerular capillaries were increased. The foot processes were destructed and show loss of uniform appearance, the glomerular basement membrane was thickened, and the fenestrations of capillary endothelium were widened (Fig. 16).

The proximal tubular cells had irregular nuclei that showed loss of their peripheral chromatin and some nuclei were shrunken. The tubular epithelial cells contained multiple cytoplasmic vacuoles. The apical brush border microvilli at the luminal side were completely lost. The tubular lumen was filled with multiple epithelial debris obliterating it (Fig. 17).
The distal tubular cells had irregular heterochromatic nuclei and some of them were shrunken. The cytoplasm revealed small and large vacuoles (Fig. 18).
The interstitium revealed multiple areas of interstitial hemorrhage around the tubules (Fig. 17).

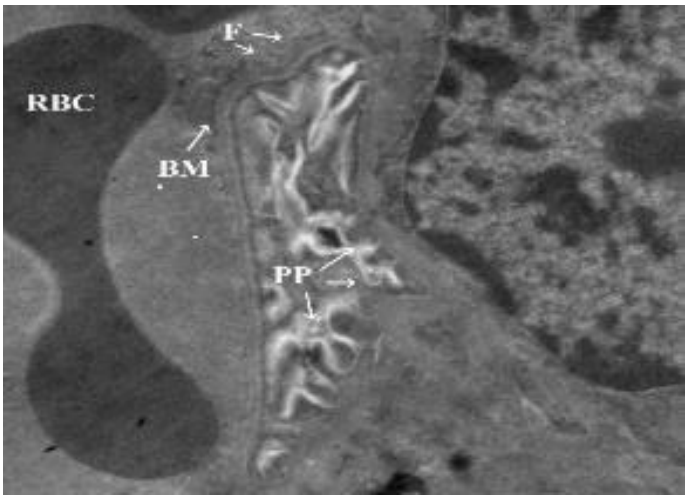

Fig. (16): Electron photomicrograph (At higher magnification) of a section in cortical part of the kidney of rat from group III showing glomerular capillary loops which contain RBCs (RBC). Some of the surrounding podocyte pedicles (PP) appear destructed with loss of uniform appearance of their foot processes. The glomerular basement membrane (BM) appears thickened The endothelial fenestrations (F) of glomerular capillary are widened. (TEM. x 20000).

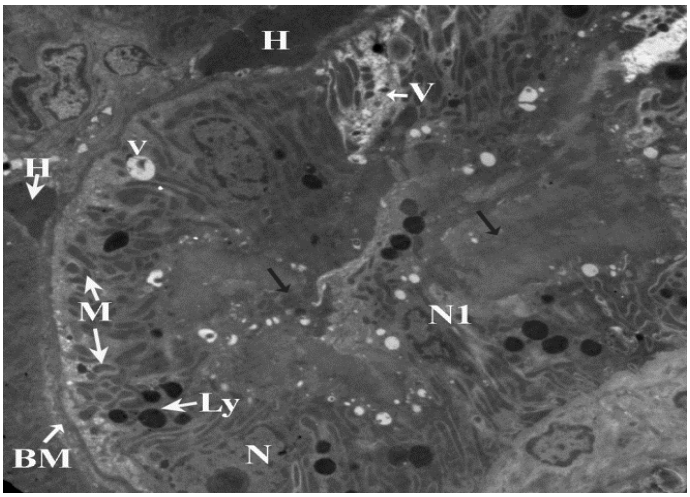

Fig. (17): Electron photomicrograph of a section in cortical part of the kidney of rat from group III showing a part of proximal convoluted tubule (P). The tubular cells have irregular nuclei (N) with loss of their peripheral chromatin and some nuclei become shrunken and apoptotic (N1). The cytoplasm containing mitochondria (M), lysosomes (Ly) and multiple vacuoles (V). The brush border microvilli at the luminal side are lost with multiple epithelial debris inside the lumen (black arrows). Around the tubules, there are multiple areas of interstitial hemorrhage (H). Basement membrane (BM) is intact. (TEM. x 4000)

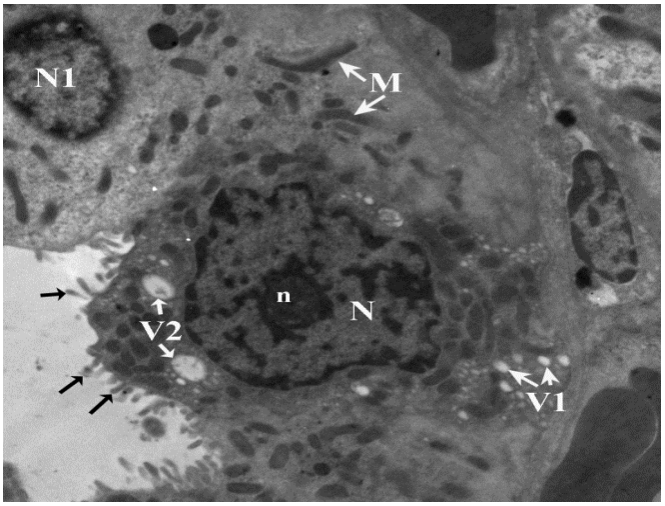

Fig. (18): Electron photomicrograph of a section in the cortical part of the kidney of rat from group III showing apart of distal tubule (D). One nucleus (N) is irregular and heterochromatic and has nucleolus (n). Another nucleus (N1) is shrunken. The cytoplasm containing small vacuoles (V1) around the nucleus in addition to large vacuoles (V2) in the apical cytoplasm and many mitochondria (M). Note: some apical microvilli are intact (black arrows) (TEM. x 10000).

Group IV:

Glomerular, tubular and interstitial alterations were increased as follows:

The glomerular capillary loops were congested with RBCs. The podocytes showed effacement of their foot processes with extensive foot processes destruction of some pedicles. The foot processes appeared broad; this might result from extensive foot processes fusion which occlude the filtration slits. The glomerular basement membrane appears thickened. The glomerular capillary endothelium showed degeneration and widening of their fenestrations (Fig. 19).

The proximal tubular cells have heterochromatic nuclei. The basement membrane is intact. Tubular epithelial cells had desquamation of epithelium and multiple cytoplasmic vacuoles. Apical brush border microvilli at the luminal side were lost at some areas and the tubular lumen showed multiple epithelial debris inside the lumen which obliterate the lumen (Fig. 20).

Most of cells of distal tubules had irregular heterochromatic nuclei and some of them were shrunken. Tubular lumen was occluded with intra-luminal cellular debris as a result of desquamation. The basement membrane is intact. The cytoplasm contained many mitochondria and multiple small vacuoles. The peritubular space showed inflammatory cellular infiltration.

Fig. (19): Electron photomicrograph of a section in cortical part of the kidney of rat from group IV showing glomerular capillary loops which contain RBCs (RBC). Some of podocytes (Pd) showing effacement of their foot processes (arrowheads) with occluded the filtration slits (FS). The glomerular basement membrane (BM) appears thickened with electron dense. There are widening of the fenestrations (F) of glomerular capillary endothelium (TEM. x 25000).

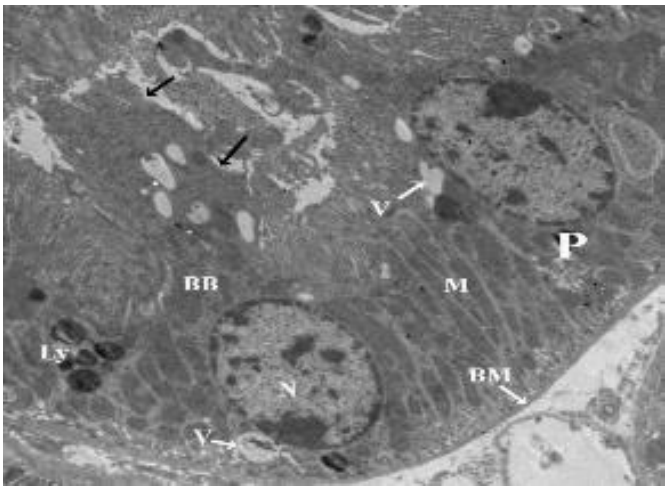

Fig. (20): Electron photomicrograph of a section in cortical part of kidney of rat from group IV showing a part of proximal convoluted tubule (P). The tubular cells have heterochromatic nuclei (N). The basement membrane (BM) is intact. The cytoplasm containing multiple vacuoles (V), many mitochondria (M) and many lysosomes (Ly). The apical brush border (BB) microvilli at the luminal side are lost at some areas. Multiple epithelial debris inside the lumen which obliterate it (black arrows) (TEM. x 6000).

Group V:

Glomerular, tubular and interstitial alterations were markedly increased as follows:

There was extensive effacement of podocytes foot processes which occlude the filtration slits, microvillus transformation of destructed pedicles, thickened glomerular basement membrane and degeneration and widening of the capillary endothelial fenestrations. The extraglomerular mesangial cells had heterochromatic irregular shaped nuclei with loss of its peripheral chromatin (Fig. 21).

The proximal tubular cells had heterochromatic nuclei. The cytoplasm contained multiple large vacuoles. The apical brush border microvilli at the luminal side were completely lost (Fig. 22).

Most of distal tubular cells were edematous and had irregular heterochromatic nuclei, some of them are shrunken or even apoptotic and the tubular lumen was contained intra-luminal cellular debris and the cytoplasm revealed extensive rarefaction and vacuolations. The peritubular space revealed hemorrhage and inflammatory cellular infiltration (Fig. 23).

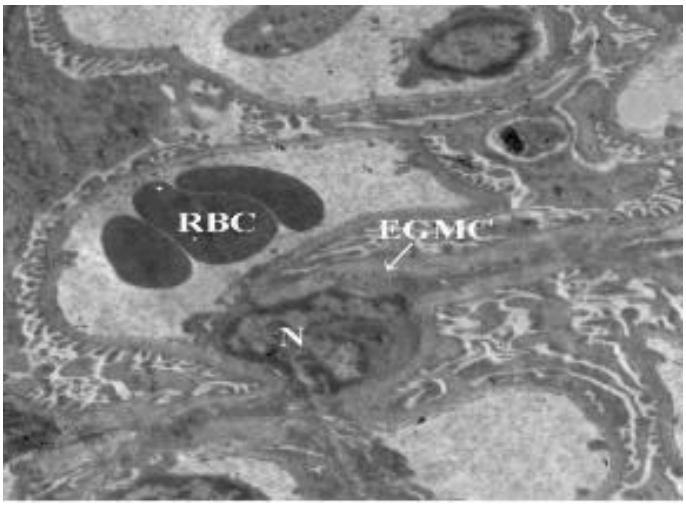

Fig. (21): Electron photomicrograph of a section in cortical part of kidney of rat from group V showing glomerular capillary loops which are congested with RBCs (RBC). The extraglomerular mesangial cell (EGMC) has heterochromatic irregular shaped nucleus (N) with loss of its peripheral chromatin (TEM. x 8000).

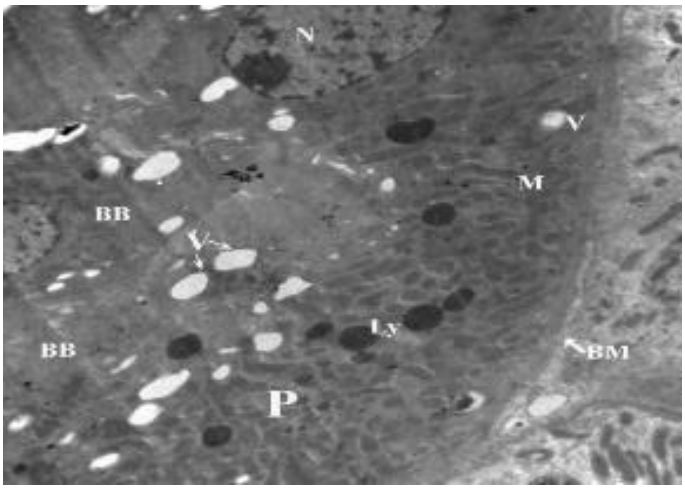

Fig. (22): Electron photomicrograph of a section in cortical part of kidney of rat from group V showing a part of proximal convoluted tubule (P). The tubular cells have heterochromatic nuclei (N). The basement membrane (BM) is thick. The cytoplasm containing multiple large vacuoles (V), many mitochondria (M) and lysosomes (Ly). The apical brush border (BB) microvilli are lost (TEM. x 6000).

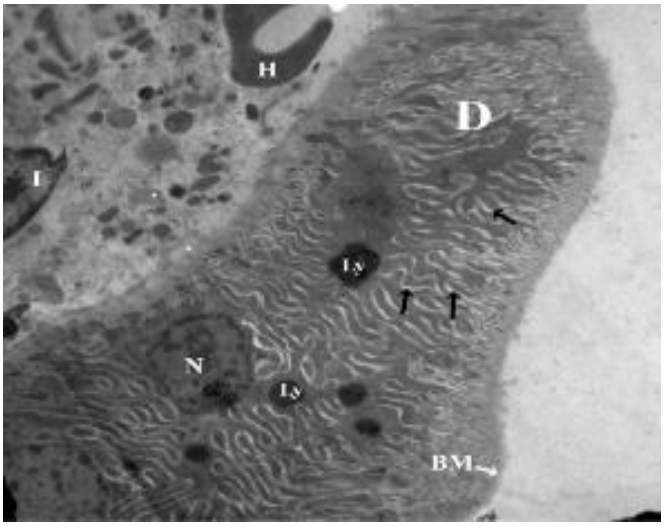

Fig. (23): Electron photomicrograph of a section in cortical part of the kidney of rat from group V showing a part of distal convoluted tubule (D). The tubular cells are edematous and have heterochromatic shrunken nuclei (N). The cells rest on thick basement membrane (BM). There is extensive cytoplasmic rarefaction and vacuolations (black arrows) and multiple lysosomes (Ly). The peritubular space show hemorrhage (H) and inflammatory cellular infiltration (I) (TEM. x 8000).

DISCUSSION

Three forms of acute kidney injury are commonly considered: prerenal, which occurs when the kidney's perfusion is diminished; renal or intrinsic; and post-renal, which occurs when there is obstruction to urine flow at any point along the tubule to urethra pathway **(8)**.

Numerous types of acute and chronic renal disorders are usually linked to drug use [2].

In the present work, the kidney was chosen as a target for toxic effect of cefepime as it was reported by **Goldstein *et al.*** **(9)** that, Cephalosporin nephrotoxicity is influenced by renal cortical accumulation and intracellular concentration.

Cefepime intramuscular injection caused significant tubular, glomerular, and interstitial changes in the rat kidney cortex and medulla. The proximal, distal and collecting tubules were affected.

The glomerular changes due to low dose of cefepime injection (up to 50 mg/kg/day) was minimal on the cortex and medulla. These changes were increased in group which received cefepime in higher concentrations (III, IV and V) which revealed multiple atrophied glomeruli with abnormal Bowman's spaces. The electron microscopic findings demonstrated podocytes foot processes effacement and destructions, occluded filtration slits, thickening of glomerular basement membrane and capillary endothelial degeneration with widening of their fenestrations. This is generally in agreement with **Paueksakon and Fogo** **(2)** who reported that significant foot processes effacement is indicative of minimum change disease and that -lactam antibiotics and cephalosporins are involved in AIN.

The present light microscopic results regarding proximal tubules clarified that all groups which received cefepime revealed edematous epithelial lining, interrupted basement membrane, some cytoplasmic vacuoles and the tubular lumina are dilated and contain intra-luminal cellular debris. Desquamation of epithelium were marked with multiple cytoplasmic vacuoles were observed in group IV and V (which received more higher concentrations of cefepime). This is in line with the findings of **Elsayed *et al.*** **(4)** who found that cefepime affect the renal tubules leading to presence of eosinophilic casts, dilatation of some tubules, and degenerative changes (cloudy swelling in the epithelial cells lining of the tubules or even complete destruction), and desquamation of epithelial cells of some tubules.

Findings from electron microscopy of the proximal tubules in the current work showed that some nuclei of tubular epithelium appeared shrunken and irregular with loss of their peripheral chromatin. The apical brush border microvilli at the luminal side were varied from lost in some areas to mostly lost. The tubular epithelial cells showed multiple focal cytoplasmic vacuoles which was more prominent in group III, IV and V with thinning of the basement membrane. There was extensive rarefaction of the cytoplasm in group V (which received cefepime in highest concentrations).

These findings are generally in agreement with **Zhou and Magi-Galluzzi** [10] who mentioned that ATN can be caused by antibiotics such as cephalosporin, aminoglycosides, amphotericin B, polymyxin B and rifampicin. Two damage patterns can be seen in the tubules. The first and most frequently observed at autopsies is coagulation necrosis of tubular cells. Cell membranes lose their distinctness, the nuclei were destructed, and cell debris may drop in the lumen. The second pattern, which is subtler, is the result of sloughing and single cell necrosis. The tubular epithelium's attenuation or flattening with widely spaced nuclei is its defining feature. The brush boundary disappears from the remaining cells. Short sections of denuded tubular basement membranes could exist.

According to this work, **Longstreth *et al.*** [11] detect localized cytoplasmic vacuolization and weakening of the basement membrane consistent with nephrotoxic acute tubular necrosis brought on by cephalexin (one of first generation cephalosporins).

On the other hand, distal tubular alterations were less than that showed in proximal tubules in light microscopic examination of all groups which received cefepime. It revealed dilated lumina with edematous epithelial lining and dropped out cells of some tubules.

These results are in the line with **Elsayed *et al.*** [4] who revealed that desquamation of tubular cells, hyaline casts in collecting tubules and cystic dilatation were all characteristics of cefepime nephrotoxicity.

The electron microscopic findings aid the light microscopic results regarding distal tubules. It demonstrated marked alterations in group III, IV and V. It showed irregular heterochromatic, some shrunken nuclei, intra-luminal cellular debris and multiple cytoplasmic vacuoles. There was extensive rarefaction of the cytoplasm in group V.

The results of the present work showed that the tubular alterations by cefepime not only confined on the cortex of the kidney but also collecting tubules in the medullary region were affected; the collecting tubules had edematous epithelial lining with cytoplasmic vacuoles and detached epithelium of some tubules as which seen in group II and were more prominent in group III, IV and V.

These results agree with **Zhou and Magi-Galluzzi** [10] who mentioned that the collecting ducts in acute tubular necrosis may contain granular casts of sloughed cells.

Regarding the interstitium, the light and electron microscopic results revealed congestion of interstitial blood vessels with patchy areas of infiltrating inflammatory cells around the tubules and focal areas of interstitial hemorrhage in group II, III, and IV that became extensive interstitial hemorrhage in group V.

These results concur with those of **Mac *et al.*** [12], who made comparable observations. They stated that a renal biopsy had shown AIN as the underlying cause of acute kidney injury, and that cefepime treatment had caused interstitial fibrosis and patchy areas of infiltrating inflammatory cells, primarily lymphocytes, plasma cells, and neutrophils.

In the same line, **Perazella and Markowitz** [13] found that acute interstitial nephritis due to drugs is characterized by significant interstitial inflammation and lymphocytes, eosinophils, and localized plasma cells.

As the cephalosporins (including cefepime) excretion is primarily by the kidney and mainly by tubular secretion [6, 14] or by glomerular filtration [15], the doses of cephalosporins must be adjusted in cases of renal dysfunction to guard against its accumulation and toxicity.

Patients and doctors will both benefit from more knowledge about cefepime therapy. The goal of this study was to examine the kidney's histological and ultrastructural changes following cefepime treatment in rats in relation to the dose used. As nephrotoxicity is a common side effect limiting the use of cefepime, it is important to note that cefepime-associated nephrotoxicity can frequently be prevented by adjusting the dose of the drug.

CONCLUSION

The results of this work revealed that intramuscular injection of cefepime led to histological and ultrastructural alterations of the rat kidney. In the cortex and medulla of the rat kidney, cefepime induced tubular, glomerular, and interstitial changes. It's obviously clear that, cefepime nephrotoxicity were marked with increasing its concentration which proves that cefepime nephrotoxicity in rats were dose related and direct cytotoxic damage to the renal tubules, glomeruli, and interstitium was observed as this antibiotic's concentration was increased.

Disclosure

In respect to the content of this paper, the authors have no financial interests to disclose.

Authorship: All authors have a substantial contribution to the article.

Fund: None.

REFERENCES

1. **Golan D, Tashjian A, Armstrong E *et al.* (2011):** Principles of Pharmacology: The pathophysiologic basis of drug therapy. 3rd edition. Section V: Principles of chemotherapy. Chapter 33: Pharmacology of bacterial infections: DNA replication, transcription, and translation. Lippincott Williams and Wilkins, Philadelphia, 581-598.
2. **Paueksakon P, Fogo A (2017):** Drug-induced nephropathies. Histopathol., 70 (1): 94-108.
3. **Tripathi K (2013):** Essentials of medical pharmacology. Seventh edition. Section 12: Antimicrobial drugs. Chapter

51: Beta-Lactam Antibiotics. Jaypee brother's medical publishers, New Delhi, 716-32.

4. **Elsayed M, Elkomy A, Gaballah M *et al.* (2014):** Nephrotoxicity of cefepime: a new cephalosporin antibiotic in rats. J Pharmacol Pharmacotherap., 5(1): 33-8.
5. **Zanetti G, Bally F, Greub G *et al.* (2003):** Cefepime versus imipenem cilastatin for treatment of nosocomial pneumonia in intensive care unit patients: A multicenter, evaluator-blind, prospective, randomized study. Antimicrobial Agents and Chemotherapy, 47: 3442-7.
6. **Rowett H (1989):** Dissection guides, part III; the rat with notes on the mouse. Second edition, John Murray. London, 5-25.
7. **Bancroft J, Layton C, Suvarna S (2012):** Theory and practice of Histological Techniques, sixth edition, Chapter 22: Transmission electron microscopy: by Wood AE and Stirling JW (Eds.). Churchill Livingstone, China, 493-538.
8. **Hobson R, Strachan M, Ralston S *et al.* (2022):** Davidson's Principles and Practice of Medicine. Twenty fourth Edition. Part 3, clinical medicine Chapter 18: Nephrology and urology. Elsevier. Churchill Livingstone, London, 557-612.
9. **Goldstein R, Pasino D and Hook J (1986):** Cephaloridine nephrotoxicity in aging male Fischer-344 rats. Toxicol., 38: 43-53.
10. **Zhou M, Magi-Galluzzi C (2007):** Genitourinary pathology. Second edition. Chapter 5: Nonneoplastic Diseases of the Kidney. Elsevier Health Sciences, China, 251-305.
11. **Longstreth K, Robbins S, Smavatkul C *et al.* (2004):** Cephalexin-induced acute tubular necrosis. Pharmacotherapy, 24(6): 808-11.
12. **Mac K, Chavada R, Paull S *et al.* (2015):** Cefepime induced acute interstitial nephritis – a case report. BMC Nephrol J., 16:15.
13. **Perazella M, Markowitz G (2010):** Drug-induced acute interstitial nephritis. Nature Reviews Nephrol., 6:461-70.
14. **Brunton L, Dandan R, Knollmann B (2018):** Goodman and Gilman's: The pharmacological basis of therapeutics. Twelfth edition. Section VII: Chemotherapy of Infectious Diseases. Chapter 57: Penicillins, Cephalosporins, and other β-Lactam Antibiotics, by: Conan MacDougall. McGraw-Hill professional, United States, 1023-38.
15. **Whalen K, Finkel R, Panavelil T (2015):** Lippincott's illustrated reviews: Pharmacology. 6th edition. Chapter 38: Cell Wall Inhibitors. Unit VII: Chemotherapeutic Drugs. Lippincott Williams and Wilkins, China, 483-97.